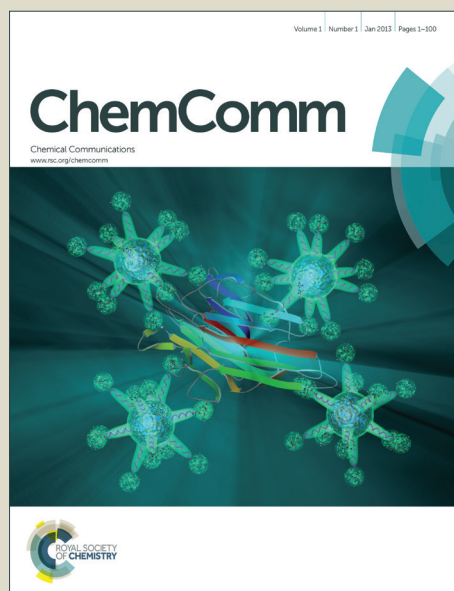


ChemComm

Accepted Manuscript



This is an *Accepted Manuscript*, which has been through the Royal Society of Chemistry peer review process and has been accepted for publication.

Accepted Manuscripts are published online shortly after acceptance, before technical editing, formatting and proof reading. Using this free service, authors can make their results available to the community, in citable form, before we publish the edited article. We will replace this *Accepted Manuscript* with the edited and formatted *Advance Article* as soon as it is available.

You can find more information about *Accepted Manuscripts* in the [Information for Authors](#).

Please note that technical editing may introduce minor changes to the text and/or graphics, which may alter content. The journal's standard [Terms & Conditions](#) and the [Ethical guidelines](#) still apply. In no event shall the Royal Society of Chemistry be held responsible for any errors or omissions in this *Accepted Manuscript* or any consequences arising from the use of any information it contains.

Cite this: DOI: 10.1039/c0xx00000x

www.rsc.org/xxxxxx

ARTICLE TYPE

A facile approach for preparation of tunable acid nano-catalyst with hierarchically mesoporous structure†

Youngbo Choi[‡], Yang Sik Yun[‡], Hongseok Park, Dae Sung Park, Danim Yun, and Jongheop Yi*

Received (in XXX, XXX) Xth XXXXXXXXX 2014, Accepted Xth XXXXXXXXX 2014

DOI: 10.1039/b000000x

A facile and efficient approach to prepare hierarchically and radially mesoporous nano-catalysts with tunable acidic properties has been successfully developed. The nanospheres show excellent catalytic performance for the acid catalysed reactions, cracking of 1,3,5-triisopropylbenzene and hydrolysis of sucrose.

Hierarchically porous nanomaterials have attracted a great deal of interest in recent years because of their superior physicochemical properties such as large surface areas, high porosity, and low density, etc.^{1,2} However, many hierarchically porous nanomaterials, such as silica, are chemically and/or catalytically inactive, making it difficult to meet the needs of these materials for practical applications including catalysis, adsorption, separation, drug delivery, and sensing.³

The incorporation of heteroatoms into the silica framework by a direct synthesis or post-grafting method has been widely used to create active sites.⁴ These conventional methods, however, suffer from some critical limitations, such as the collapse of their structure when a large amount of heteroatoms are introduced,⁵ complex and time-consuming process,^{3,6} and difficulty to control the amount of grafted heteroatoms.⁷ Therefore, the development of simple and efficient strategies for preparing the hierarchically porous nanomaterials with adjustable catalytic functionalities continues to be a great challenge.

Herein, we report on a convenient and effective route for preparing tunable acid nano-catalysts with hierarchically and radially mesoporous structure. In this method, referred to as “pH-assisted delay addition”, an Al precursor was added to a pH adjusted solution containing preformed hierarchically and radially mesoporous (HRM) nanostructures via a hydrothermal treatment.² A second hydrothermal treatment was then used to introduce heteroatoms into the silica framework, resulting in maintaining the unique structure with acid properties. In contrast, when a small amount of Al precursor was included in the initial solution, as in the case of the direct synthesis, HRM nanostructures were not obtained (Fig. S1).

In the developed procedure, it is noteworthy that the reaction time required to preform the HRM nanostructure and the pH shift prior to the addition of the Al precursor played a crucial role in introducing the functionality while maintaining its nanostructures (Fig. S1). Interestingly, by simply changing the pH adjusting agent in the procedure to prepare the aluminosilicate nanospheres

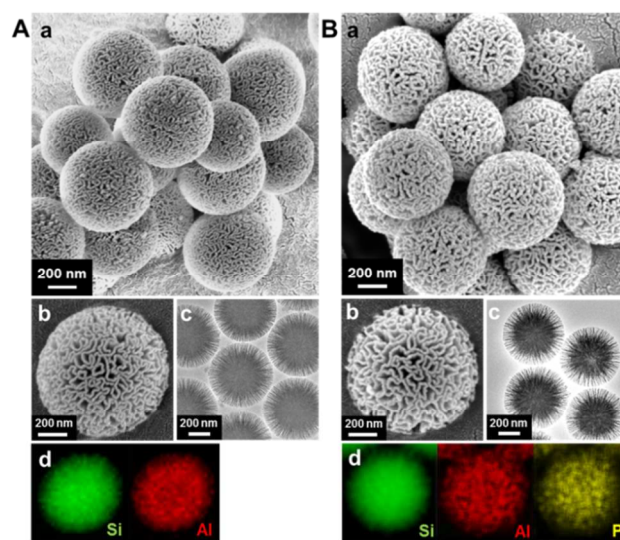


Fig. 1 (a, b) SEM, (c) TEM, and (d) EDS mapping images of (A) ASN-40 and (B) ASPN-40 samples.

(denoted as ASN-X where “X” indicates the Si/Al molar ratio), we can induce incorporation of P as well as Al into silica framework, leading to formation of aluminosilicophosphate nanospheres (denoted as ASPN-X where “X” indicates the Si/Al molar ratio). Furthermore, Si/Al ratio of the both ASN and ASPN samples can be easily controlled by simply changing the concentrations in the initial preparation solution because its ratios in the preparation solution were preserved in the final samples while the content of P in the ASPN samples is about half that of the Al (Table S1).

The morphology and structure of ASN and ASPN samples with various Si/Al ratios prepared under optimum conditions were investigated by electron microscopy. As shown in the scanning electron microscopy (SEM) images, both ASN and ASPN samples are spherical in shape with a uniform particle size (450-600 nm) (Fig. 1a,b and Fig. S2). Magnified SEM images demonstrate that the wrinkled sheets are arranged in three dimensions to form a spherical shape with a pore mouth size of 15-50 nm. The large diameters of the pores can permit guest molecules to easily access the active sites inside the pores. The transmission electron microscopy (TEM) images indicate that the pores are radially oriented, and their size gradually increases from the center to the outer surface (Fig. 1c and Fig. S2). Elemental

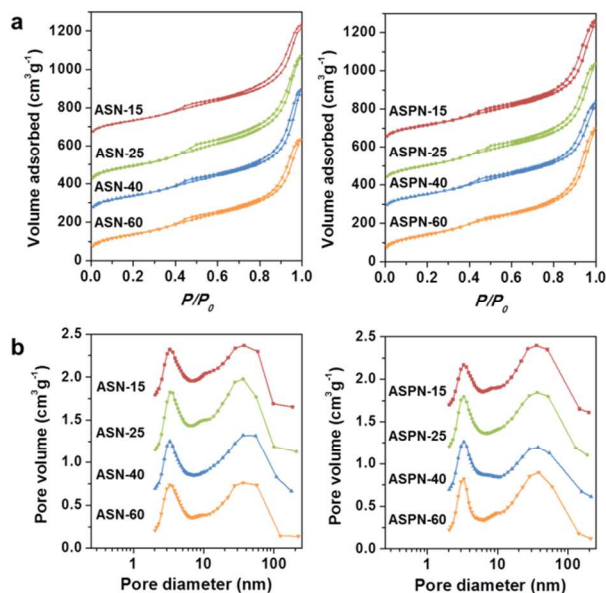


Fig. 2 (a) N_2 adsorption-desorption isotherms and (b) BJH adsorption pore size distribution curves of ASN and ASPN samples with different Si/Al molar ratios

5 mapping images demonstrate a highly homogeneous distribution of elemental Si and Al in the ASN, and elemental P as well as Si and Al in the ASPN samples (Fig. 1d), suggesting the effective formation of acid sites.

The porous structure of the ASN and ASPN samples was further evaluated by N_2 adsorption-desorption measurements. All ASN samples exhibited a type IV isotherm with a H3 type hysteresis loop in the relative pressure range of 0.4-1.0, implying the presence of various sized, slit-shaped mesopores (Fig. 2a).⁸ The BJH adsorption pore volume curves further confirm these multimodal pore size distributions, which consist of a relatively sharp peak (3 nm), a feeble shoulder peak (10 nm) and a broad peak (37 nm) (Fig. 2b). Interestingly, although ASN and ASPN samples were prepared using a wide range of Si/Al ratios and different Al/P ratios, they all had a uniform pore structure and very similar surface areas ($511 \pm 32 \text{ m}^2 \text{ g}^{-1}$) (Fig. 2 and Table S2). This textural uniformity of ASN and ASPN particles across the various compositions clearly demonstrates that the pH-assisted delayed addition method can overcome the limitations of conventional functionalization methods, in which the incorporation of a functionality generally leads to a decrease in textural and structural properties.³

The acid and ion exchange sites of aluminosilicate materials are mainly associated with a tetrahedrally coordinated Al in the framework.^{9,10} ^{27}Al MAS NMR analysis revealed the coordination environment of the Al (Fig. S3). All ASN samples showed a strong peak (51-56 ppm) corresponding to a tetrahedrally coordinated Al in the framework and a weak peak (0 ppm) attributed to an octahedrally coordinated Al in the extra-framework,^{10,11} suggesting that most of the Al species are incorporated into the framework. Indeed, the proportion of tetrahedral Al, estimated from the relative intensities of the NMR peaks,^{10,11} exceeded 70 % for all ASN samples (Table S2). Moreover, the proportion of tetrahedral Al in ASN-40 was about 1.5 times higher than the corresponding values for a commercial mesoporous aluminosilicate AIMCM-41 with the same Si/Al

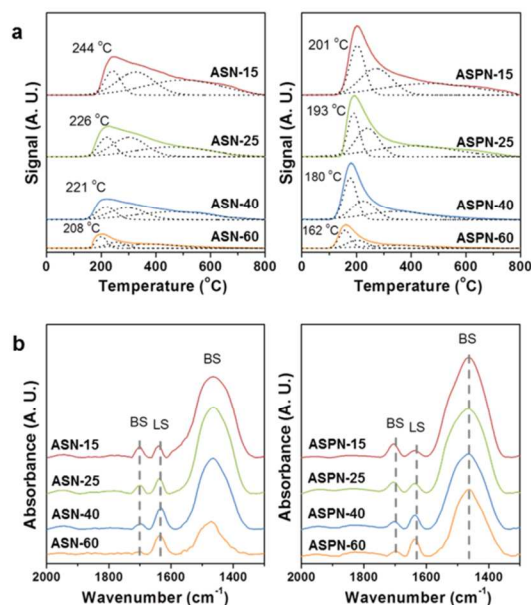


Fig. 3 (a) NH_3 -TPD curves and (b) *in situ* FTIR spectra for adsorbed NH_3 of ASN and ASPN samples with different Si/Al molar ratios. Peak assignments in FTIR spectra; 1640 cm^{-1} (Lewis acid sites: LS), 1470 and 1705 cm^{-1} (Brønsted acid sites: BS)

ratio of 40 (Table S2). In case of ASPN samples, the spectra were similar to those previously reported for mesoporous aluminosilicophosphates, indicating the presence of tetrahedral and octahedral atoms which are bonded with P atoms via oxygen bridges.¹² These findings demonstrate that the developed method has a high efficiency for incorporating heteroatoms and creating acid sites.

The amount and strength of the acid sites on the ASN and ASPN samples were evaluated by the temperature-programmed desorption (TPD) of NH_3 . To reveal the distribution of acid strength, the TPD curves were fitted by Gaussian deconvolution¹³ (Fig. 3a and Table S3). The total amount of acid sites progressively increased with increasing Al content, from $0.132 \text{ mmol g}^{-1}$ for ASN-60 to $0.609 \text{ mmol g}^{-1}$ for ASN-15. The peak maximum of the TPD curves shifted to higher temperatures with increasing Al content, indicating an increase in acid strength. The acid strength distribution also showed a positive relation between Al content and densities for both medium and strong acidity. As compared with the ASN samples with the same Si/Al ratio, the total acid amount on the ASPN samples was significantly increased. In order to distinguish between Brønsted and Lewis acid sites on the samples, *in situ* FTIR spectra for NH_3 adsorbed on the samples were also recorded (Fig. 3b and Table S3). In the spectra, two bands at ca. 1470 and 1705 cm^{-1} are assigned to NH_3 adsorbed on Brønsted acid sites, and a band at 1640 cm^{-1} is attributed to NH_3 adsorbed on Lewis acid sites.¹⁴ The ratio of Brønsted to Lewis acid sites (BS/LS ratio) on the ASN samples was gradually enhanced with increasing Al content, from 0.6 for ASN-60 to 5.5 for ASN-15. In the case of the ASPN samples, the BS/LS ratio was noticeably increased compared to the ASN samples with the same Si/Al ratio. These larger acid amount and higher BS/LS ratio of the ASPN samples can be attributable to OH groups associated with P atoms which provide additional weak Brønsted acid sites.^{9,15}

80 Compared with AIMCM-41, the total amount of acid and the

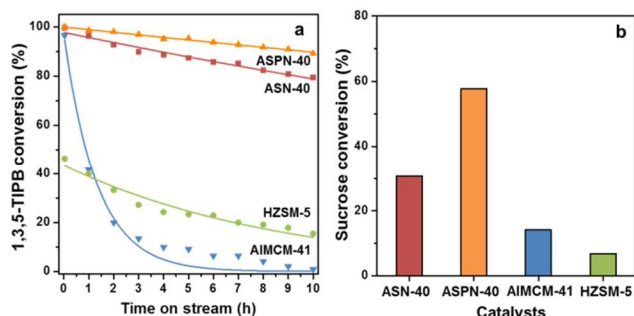


Fig. 4 (a) Time course for 1,3,5-TIPB conversion and (b) sucrose conversion over ASN-40, ASPN-40, AIMCM-41, and HZSM-5. Each line in (a) indicates a fitted curve by the first order deactivation model.

ratio of Brønsted to Lewis acid sites (BS/LS ratio) in ASN-40 were higher by 1.8 and 1.7, respectively (Fig. S4 and Table S3). In amorphous aluminosilicates such as ASN and AIMCM-41 (Fig. S5), the Brønsted acidity originates from silanol groups, which are strongly influenced by neighboring Al atoms.¹⁶ As shown in Fig. 1d, our method results in the highly homogeneous distribution of Si and Al atoms, which facilitates the creation of silanol groups having neighboring Al, which serves to enhance the acidity.

The catalytic performance of the ASN and ASPN samples was evaluated in two acid-catalysed reactions (Fig. 4). The cracking of 1,3,5-triisopropylbenzene (1,3,5-TIPB) and the hydrolysis of sucrose were chosen as model reactions for the transformation of a hydrocarbon and biomass, respectively. By different product distributions of 1,3,5-TIPB cracking and conversions of sucrose over the samples, tunable acidic properties of ASN and ASPN samples were confirmed (Table S4). To demonstrate the versatility of ASN and ASPN catalysts, AIMCM-41 and HZSM-5 with the same Si/Al ratio of 40 were also tested. In the cracking of 1,3,5-TIPB, HZSM-5 showed the lowest activity, since 1,3,5-TIPB is too large to enter the pores of the HZSM-5 and the reaction only occurs on the external surface.¹⁷ AIMCM-41 showed a high initial activity, but was deactivated rapidly. Interestingly, ASN-40 and ASPN-40 not only exhibited a higher activity, but also retained much longer life time than the reference catalysts due to high coke resistance originated from their unique pore structure and proper acidity (Fig. S6).¹⁸ The deactivation rate constant calculated from the first order deactivation model¹⁹ was in the order of ASPN-40 (0.01 h^{-1}) < ASN-40 (0.02 h^{-1}) < HZSM-5 (0.11 h^{-1}) << AIMCM-41 (0.75 h^{-1}). Furthermore, ASN-40 was revealed to be more stable in terms of hydrothermal stability than AIMCM-41, exhibiting a relatively high activity and maintaining its structure (Fig. S7 and Table S5). In the hydrolysis of sucrose, ASN-40 and ASPN-40 showed a higher performance than the reference catalysts (Fig. 4b). In particular, the conversion of sucrose over ASPN-40 was more than 4 times that of AIMCM-41 and HZSM-5, mainly due to the high content and easy accessibility of the Brønsted acid sites in ASPN-40.²⁰

In summary, we report on an attractive route for introducing tunable acidic properties into the hierarchical mesoporous nanospheres. These procedures permit the amount, types, and strength of acid sites to be precisely adjusted. These are important properties for solid-acid, and textural uniformity can be maintained across various compositions. The excellent catalytic properties of the resulting nanospheres suggest that they have

great potential for use as solid acids in chemical industry and expand the scope of hierarchically structured nanomaterials.

This subject is supported by Korea Ministry of Environment as “Converging technology project (202-091-001)”.

Notes and references

- ⁵⁵ World Class University Program of Chemical Convergence for Energy & Environment, Institute of Chemical Processes, School of Chemical and Biological Engineering, College of Engineering, Seoul National University, Seoul 151-742, Republic of Korea. E-mail: jyi@snu.ac.kr; Tel: +82-2-880-7438
- ⁶⁰ †Electronic Supplementary Information (ESI) available: Experimental details, characterization (EPMA, SEM and TEM images, XRD spectra, NH_3 -TPD, *in situ* FTIR spectra of adsorbed NH_3 , ^{27}Al MAS NMR spectra N_2 adsorption-desorption isotherms, and TG analysis), catalytic activities for the cracking of 1,3,5-TIPB and hydrolysis of sucrose, and hydrothermal stability test. See DOI: 10.1039/b000000x/
- ⁶⁵ ‡ These authors contributed equally.
- 1 X. Du and J. He, *Nanoscale*, 2011, **3**, 3984; W. C. Yoo and A. Stein, *Chem. Mater.*, 2011, **23**, 1761; H. Zhang, Z. Li, P. Xu, R. Wu and Z. Jiao, *Chem. Commun.*, 2010, **46**, 6783; X. Du and J. He, *Langmuir*, 2010, **26**, 10057.
- 2 V. Polshettiwar, D. Cha, X. Zhang and J. M. Basset, *Angew. Chem., Int. Ed.*, 2010, **49**, 9652; D. S. Moon and J. K. Lee, *Langmuir*, 2012, **28**, 12341.
- 3 N. Linares, E. Serrano, M. Rico, A. M. Balu, E. Losada, R. Luque and J. García-Martínez, *Chem. Commun.*, 2011, **47**, 9024.
- 4 J. Y. Ying, C. P. Mehnert and M. S. Wong, *Angew. Chem., Int. Ed.*, 1999, **38**, 56; A. Corma, V. Fornés, M. T. Navarro, J. Pérez-Pariente, *J. Catal.*, 1994, **148**, 569; R. Mokaya and W. Jones, *Chem. Commun.*, 1997, 2185.
- 5 L. Li, J. L. Shi, L. X. Zhang, L. M. Xiong and J. N. Yan, *Adv. Mater.*, 2004, **16**, 1079; S. Wu, Y. Han, Y. C. Zou, J. W. Song, L. Zhao, Y. Di, S. Z. Liu and F. S. Xiao, *Chem. Mater.*, 2004, **16**, 486.
- 6 A. Ungureanu, B. Dragoi, V. Hulea, T. Cacciaguerra, D. Meloni, V. Solinas, E. Dumitriu, *Microporous Mesoporous Mater.*, 2012, **163**, 51.
- 7 Z. Luan, M. Harmann, D. Zhao, W. Zhou and L. Kevan, *Chem. Mater.*, 1999, **11**, 1621; Z. Luan, E. M. Maes, P. A. W. van der Heide, D. Zhao, R. S. Czernuszewicz and L. Kevan, *Chem. Mater.*, 1999, **11**, 3680; Z. Luan, J. Y. Bae and L. Kevan, *Chem. Mater.*, 2000, **12**, 3202.
- 8 K. S. W. Sing, D. H. Everett, R. A. W. Haul, L. Moscou, R. A. Pierotti, J. Rouquéro and T. Siemieniowska, *Pure Appl. Chem.*, 1985, **57**, 603.
- 9 A. Corma, *Chem. Rev.*, 1995, **95**, 559.
- ⁹⁵ 10 R. Mokaya, *Chem. Commun.*, 2000, 1891.
- 11 A. Yin, X. Guo, W. L. Dai and K. Fan, *J. Phys. Chem. C*, 2010, **114**, 8523.
- 12 T. D. Conesa, R. Mokaya, J. M. Campelo and A. A. Romero, *Chem. Commun.*, 2006, 1839; X. S. Zhao, G. Q. Lu, A. K. Whittaker, J. Drennan and H. Xu, *Microporous Mesoporous Mater.*, 2002, **55**, 51.
- 13 D. Li, F. Li, J. Ren and Y. Sun, *Appl. Catal., A*, 2003, **241**, 15.
- 14 C. C. Hwang and C. Y. Mou, *J. Phys. Chem. C*, 2009, **113**, 5212; Y. Choi, D. S. Park, H. J. Yun, J. Baek, D. Yun and J. Yi, *ChemSusChem*, 2012, **5**, 2460.
- ¹⁰⁵ 15 H. O. Pastore, S. Coluccia and L. Marchese, *Annu. Rev. Mater. Res.*, 2005, **35**, 351.
- 16 J. Huang, N. V. Vegten, Y. Jiang, M. Hunger and A. Baiker, *Angew. Chem., Int. Ed.*, 2010, **49**, 7776.
- 17 T. Hibino, M. Niwa and Y. Murakami, *J. Catal.*, 1991, **128**, 551.
- ¹¹⁰ 18 Z. Qin, B. Shen, X. Gao, F. Lin, B. Wang and C. Xu, *J. Catal.*, 2011, **278**, 266; P. D. Hopkins, J. T. Miller, B. L. Meyers, G. J. Ray, R. T. Roginski, M. A. Kuehne and H. H. Kung, *Appl. Catal., A*, 1996, **136**, 29.
- 19 H. Mochizuki, T. Yokoi, H. Imai, S. Namba, J. N. Kondo and T. Tatsumi, *Appl. Catal., A*, 2012, **449**, 188; W. H. Chen, S. J. Huang, Q. Zhao, H. P. Lin, C. Y. Mou and S. B. Liu, *Top. Catal.*, 2009, **52**, 2.
- 20 C. Tagusagawa, A. Takagaki, A. Iguchi, K. Takanabe, J. N. Kondo, K. Ebitani, T. Tatsumi and K. Domen, *Chem. Mater.*, 2010, **22**, 3072.